

**EFFECT OF THE HEIGHT OF A MELTED LAYER ON ITS THERMAL STRUCTURE
IN GROWING SINGLE CRYSTALS BY THE STOCKBARGER METHOD
WITH THE USE OF THE ACCELERATED CRUCIBLE ROTATION TECHNIQUE**

V. É. Distanov and A. G. Kirdyashkin

UDC 532.5+536.25+548.5

The effect of the height of a melted layer on its thermal structure is examined. The maximum velocities of ascending and descending flows during crystal growth by the Stockbarger method with the use of the accelerated crucible rotation technique in crucibles 100 mm in diameter at Taylor numbers $Ta > 10^8$ are estimated. A sudden increase in the amplitude of temperature oscillations with diminution of the height of the melted layer caused by unsteady rotation of the crucible is found. With decreasing height of the melted layer, the velocity of both ascending and descending flows at the axis of a cylindrical ampoule decreases.

Introduction. The accelerated crucible rotation technique (ACRT) developed by Scheel and Schulz-DuBois [1–3] is widely used for single-crystal growth of a wide class of compounds by various methods (the Stockbarger and Czochralski methods, solution-melt growth, zone melting, etc.). A number of works dealing predominantly with the computational aspect of the problem were devoted to the elucidation of various features of hydrodynamic and thermal processes proceeding in the melt during crystal growth by the ACRT, being aimed at optimization of the crystallization process [3–13]. However, the effect of the height of the melted layer on its hydrodynamic and thermal structure was addressed rather scarcely [5, 9, 13], especially for the case of crystallization in crucibles of large diameter at Taylor numbers

$$Ta = (\omega_{\max}^2 - \omega_0^2)r^4/\nu^2 > 10^8,$$

where ω_{\max} and ω_0 are the maximum and mean angular velocities of the rotating crucible, r is its inner diameter, and ν is the kinematic viscosity.

In the present work, we model variation of the thermal structure of the melted layer with its height during growth of single crystals by the Stockbarger method using the ACRT. Model tests are performed, and the thermal structure of the model liquid (96% ethanol) is considered for Prandtl numbers $9.7 < Pr < 10.8$ ($Pr = \nu/a$, where a is the thermal diffusivity of the liquid) for a crucible 100 mm in diameter rotating with a modulated velocity around the vertical axis.

The results of model experiments were used to optimize the growth conditions for single crystals from acoustooptic and nonlinear materials [$Pr = 0.38$ [14] for proustite (Ag_3AsS_3) and $Pr = 8.57$ [15, 16] for lead bromide ($PbBr_2$)] in the Stockbarger procedure with unsteady rotation of the container. The velocity and pressure fields in this procedure depend on the proportion between centrifugal and frictional forces, i.e., the Taylor number. Both in model studies and in actual growth of proustite and lead bromide crystals, identical values of Ta were used. In modeling the growth of lead bromide crystals from the melt, we used ethanol, taking full advantage of the fact that the kinematic viscosities of both materials are identical, whereas their Prandtl numbers are very close. The value of Pr for proustite is smaller than that for ethanol, and the

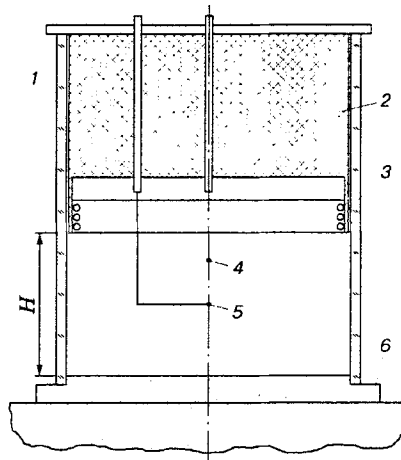


Fig. 1. Scheme of the experimental setup: 1) quartz crucible; 2) fluoroplastic cylindrical shutter; 3) heater; 4) central thermocouple; 5) L-shaped thermocouple; 6) isothermal base.

thickness of the thermal boundary layer near the crystallization front for proustite is greater than that near the thermally insulated base imitating the growing crystal in model studies with ethanol. However, for the most part, the similarity conditions for the velocity and pressure fields were satisfied.

Experimental Procedure. The thermal structure of the crucible was experimentally studied using a setup for which the law of unsteady rotation of the table with a fixed crucible could be varied from the saw-tooth to the trapezoidal one. The control system could ensure an arbitrary proportion between the rates of increasing and decreasing angular velocity and the time intervals with constant maximum and minimum values of the angular velocity n . The direction of crucible rotation could be changed. With the help of sliding contacts, the temperature in the crucible was measured simultaneously with eight thermocouples. The error in measurements of the e.m.f. was $2 \mu\text{V}$. Two independent lines supplying power to the rotating table with the crucible were provided. The unchanged temperature of the substrate ("crystal") mounted on the rotating table was ensured by sliding inputs of thermally insulated water. The direction of table rotation could be varied from the vertical to the horizontal one.

The scheme of the setup is shown in Fig. 1. Cylindrical crucible 1 made from an optical-quartz tube with a 100-mm inner diameter was aligned co-axially with the vertical axis of revolution. To ensure the desired structure of the temperature field in the bulk of the model liquid, a fluoroplastic cylindrical shutter 2 with a resistive heater 3 made in the form of a double-wound 0.2 mm-wire spiral embedded into the shutter was introduced into the crucible. The height of the heater was 10 mm, and its resistance was 22Ω . The upper coil of the spiral was located 10 mm below the free surface of the liquid. The heat exchanger thus formed did not introduce any additional hydrodynamic disturbances during unsteady rotation of the crucible. It also enabled one to easily change the liquid-layer height in the crucible by raising or lowering the fluoroplastic cylinder. The temperature in the liquid bulk was measured by central (4) and L-shaped (5) differential Nichrome-Constantan thermocouples $50 \mu\text{m}$ in diameter introduced into the openings of the fluoroplastic cylinder. The cold junctions of the thermocouples were mounted on a thermally insulated copper base 6 of the quartz crucible, which was also located on the rotating table. In the experiments, the difference ΔT between the temperature of the liquid bulk and the temperature of the water-cooled bottom of the quartz crucible was measured. The flow pattern in the model liquid remained unchanged by introducing either an axial needle-like probe or an L-shaped needle-type temperature probe 0.05 mm thick with a 20 mm-long free end that was not covered by insulating capillaries. The error in the temperature measurements was $\pm 0.05^\circ\text{C}$. The electric power consumed by the heater was 10.2 W, and the substrate temperature was 24.5°C .

In the model study of the thermal structure of the melt during crystal growth by the Stockbarger

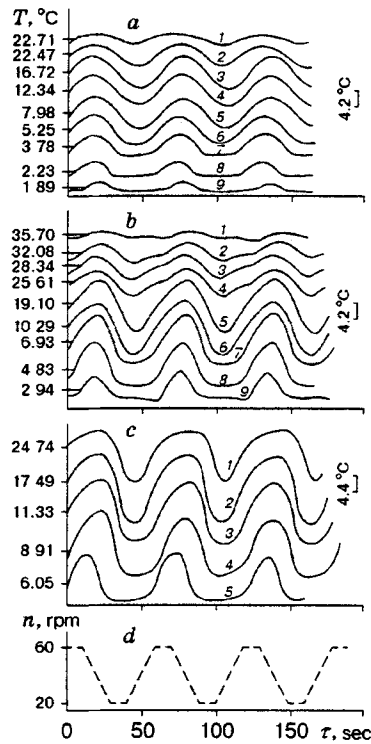


Fig. 2. Instantaneous values of the temperature at the crucible axis vs time (a-c) and the law of rotational velocity (d): (a) $H = 52$ mm; curves 1-9 refer to $y = 50.17, 45.85, 39.33, 31.03, 25.42, 18.35, 12.89, 6.80,$ and 2.06 mm, respectively; (b) $H = 37.1$ mm; curves 1-9 refer to $y = 34.85, 31.03, 28.30, 24.96, 19.20, 14.24, 10.07, 6.69,$ and 2.28 mm, respectively; (c) $H = 18$ mm; curves 1-5 refer to $y = 15.11, 12.02, 9.79, 6.54,$ and 2.26 mm, respectively.

method, the annular heater in the model ampoule, as well as the annular heater of the diaphragm of the growth furnace, ensured a constant temperature difference between the heater and the substrate, whereas the substrate imitated the planar crystallization front.

The influence of the melt height on heat transfer was studied in a liquid layer enclosed between the annular heater and the thermally insulated planar base. The free level of the model liquid was 10-12 mm above the upper level of the annular heater, and this region was isothermal both during rotation of the melt and under conditions without rotation. According to Distanov and Kirdyashkin [13], temperature oscillations induced by unsteady rotation of the crucible completely vanish in this region. Hence, in the absence of radial temperature gradients, the influence of the thermocapillary effect on the convection in the working zone of the melt is insignificant.

The position of the thermocouple junction was determined with the help of a V-630 cathetometer mounted on a coordinate table. The cathetometer permitted measurement of horizontal displacements of the junction with an accuracy of 0.01 mm. Synchronous measurements of instantaneous values of the e.m.f. generated by thermocouples and the number of revolutions of the crucible around the vertical axis (in one time scale) were ensured by a measuring complex described in [9, 13].

Results and Their Discussion. In the experiments, the Taylor number was $Ta = 1.8 \cdot 10^8$. The law of the rotational velocity of the crucible is shown in Fig. 2d. The variation of the temperature at the crucible axis (Fig. 2a-c) was similar to that of the rotational velocity. A decrease in the height H of the "working" layer resulted in a greater amplitude of temperature oscillations induced by unsteady rotation. As the height of the "working" layer decreased from 52 mm to 37.1 and 18 mm (i.e., by a factor of 2.9), the amplitude of temperature oscillations at the crystallization front increased from 2.9°C (curve 9 in Fig. 2a) to

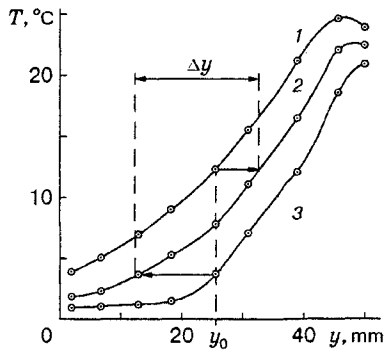


Fig. 3

Fig. 3. Distribution of the maximum, mean, and minimum temperatures (curves 1-3, respectively) over the height of the melted layer $H = 52$ mm.

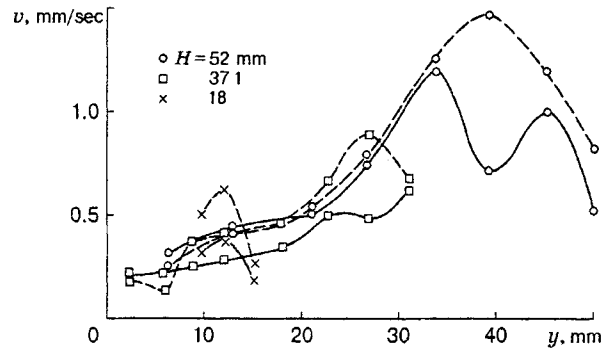


Fig. 4

Fig. 4. Distribution of the maximum velocity of the ascending (dashed curves) and descending flows (solid curves) over the height of the melted layer.

7.77°C (curve 9 in Fig. 2b) and 13.86°C (i.e., by 4.8 times) (curve 5 in Fig. 2c), respectively. For all values of H , the amplitude of temperature oscillations increased with distance from the base of the crucible, and its maximum value roughly equaled the height of the developed vortex flow. The temperature averaged over the height of the layer of the model liquid at the crucible axis obeys an exponential law (both in situations with and without unsteady rotation). Previously, a similar phenomenon was observed in experiments with crucibles of smaller diameter [9]. The unsteady rotation causes only an insignificant increase in the mean temperatures, whereas the change in the temperature averaged over the height of the flow core in situations with and without unsteady rotation is determined by heat removal along the crucible walls.

The maximum values of the ascending and descending flows at the crucible axis were estimated under the assumption that the change in temperature due to thermal conduction is substantially smaller than that due to convection. In this case, for fixed values $y = y_0$, the axial velocity can be estimated from the relation

$$v_{\max} = \left(\frac{\partial T}{\partial \tau} \right)_{\max} / \left(\frac{\partial T}{\partial y} \right)_{y=y_0},$$

where T is the temperature averaged over the height of the melted layer and τ is the time. The value of v_{\max} can be evaluated from the relation $v_{\max} = \Delta y / \Delta \tau$, where Δy is the distance covered by a particle moving along the crucible axis during the time interval $\Delta \tau$. From the T vs. τ dependence (Fig. 2a-c), we evaluated the time $\Delta \tau$ during which the temperature changed from T_{\max} to T_{\min} for fixed values of y_0 . The values of T_{\max} and T_{\min} for a given y_0 can be determined from the curves $T_{\max}(y)$ and $T_{\min}(y)$, and then Δy can be found from the mean-temperature profile $T(y)$ as shown in Fig. 3. The predicted values of v_{\max} agree well with the values of v_{\max} experimentally measured in [14] under identical test conditions. As the model liquid in [14], 96% ethanol was also used with aluminum particles several micrometers in diameter added to the mixture to visualize the flow.

Figure 4 shows the velocities of the ascending and descending flows for various heights of the “working” liquid layer contained between the heater and the thermally insulated substrate. As the height of the liquid layer decreases from 52 mm to 37.1 and 18 mm, the maximum velocity of the ascending flow decreases from 1.47 mm/sec to 0.89 and 0.62 mm/sec, and the maximum velocity of the descending flow diminishes from 1.2 mm/sec to 0.62 and 0.39 mm/sec, respectively.

With H decreased by a factor of 2.9, the maximum flow velocity decreases approximately by a factor of 2.4 and 3.1 for the ascending and descending flows, respectively. According to [9], in a similar model experiment, a more abrupt decrease in the flow velocities with decreasing layer height was observed in the case of 29-mm crucibles and $Ta \sim 10^6$ (with H decreased by four times, an eightfold decrease in the maximum velocity of the ascending flow was observed). The slower change in the flow velocities with decreasing layer

height in 100-mm crucibles compared to the case of 29-mm containers is caused by the comparatively weak decrease in the dynamic inertia of the liquid under the experimental conditions adopted in these experiments.

In our previous studies [13], the high optical quality of single crystals grown from the melt by the Stockbarger method could be ensured only if the crystallization front was located below the diaphragm's annular heater. In this case, the entire melt bulk at the beginning of crystallization can be conventionally divided into three zones: a working zone (between the crystallization front and the lower butt-end of the diaphragm's annular heater), a transitional one (where the annular heater is mounted), and a stable-temperature zone (leveled with the upper heater). With crystallization proceeding, the proportion between the heights of the above zones changes. The experiments showed that periodic temperature oscillations induced by unsteady rotation of the container arise only in the working zone, and they rapidly decay in the transitional region. In the free zone of the melt, they completely vanish [13]. At the initial stage of crystallization, the time evolution of the working-zone temperature is identical for different heights of the melted layer. As the free level of the melt descends below the diaphragm's heater, the amplitude of temperature oscillations abruptly increases. Simultaneously, the axial flow velocities in the melt decrease. At the final stage of crystallization, where the height of the melted layer is smaller than the distance from the diaphragm's heater to the crystallization front, an increase in temperature gradients and a decrease in the heat-transfer rate result in a worsened structure of the crystal in its end part owing to higher thermoelastic stresses arising in the crystal and worse mixing of the melt. The latter was also observed during the growth of proustite single crystals by the Stockbarger method using the ACRT with weak stirring of the melt [14]. Thus, the modeling of hydrodynamics and heat transfer at different heights of the melted layer allows one to elucidate the reasons for the worsened structure of crystals at the final stage of their growth and to optimize the growth conditions.

Conclusions. The model experiments showed that the mean temperature in the melt core in 100-mm crucibles at $Ta = 1.8 \cdot 10^8$ follows an exponential law and depends on heat removal along the crucible walls. The unsteady rotation of the crucible results in only an insignificant increase in the mean temperature. As the height of the melted layer decreases, the amplitude of temperature oscillations increases dramatically. The latter is caused by the change in the rotational velocity. The maximum amplitude of temperature oscillations is observed for a height comparable with the characteristic spatial scale of the developed vortex flow. The maximum values of the velocities of ascending and descending flows at the crucible axis were found to vary in proportion to the height of the melted layer. In 100-mm ampoules, the decrease in these velocities is less pronounced compared to the case of 29-mm containers. As in model experiments, a decrease in the height of the melted layer in the course of crystallization (as the melt is consumed by the growing crystal) leads to restructuring of both the temperature pattern of the melt and the velocity field in it. Hence, to maintain these parameters constant, the hydrodynamic conditions should be varied during crystallization in compliance with both the law of variation of the rotational velocity of the crucible and the absolute value of this velocity.

This work was supported by the Russian Foundation for Fundamental Research (Grant No. 98-05-65196).

REFERENCES

1. H. J. Scheel and E. O. Schulz-DuBois, "Flux growth of large crystals by the accelerated crucible rotation technique," *J. Crystal Growth*, **8**, 304-306 (1971).
2. E. O. Schulz-DuBois, "Accelerated crucible rotation: hydrodynamics and stirring effect," *J. Crystal Growth*, **12**, 81-87 (1972).
3. H. J. Scheel, "Accelerated crucible rotation: a novel stirring technique in high-temperature solution growth," *J. Crystal Growth*, **13/14**, 560-565 (1972).
4. A. Horowitz, M. Goldstein, and Y. Horowitz, "Evaluation of the spin-up time during the accelerated crucible rotation technique," *J. Crystal Growth*, **61**, 317-322 (1983).
5. P. Capper, J. J. Gosney, C. L. Jones, and E. J. Pearce, "Fluid flows induced in tall narrow containers by ACRT," *J. Electron. Mater.*, **15**, No. 6, 361-370 (1986).

6. J. C. Brice, P. Capper, C. L. Jones, and J. J. G. Gosney, "ACRT: A review of models," *Progr. Crystal Growth Charact.*, **13**, 197–229 (1986).
7. R. T. Gray, M. F. Larrousse, and W. R. Wilcox, "Diffusional decay of striations," *J. Crystal Growth*, **92**, 530–542 (1988).
8. M. F. Larrousse and W. R. Wilcox, "Interfacial mass transfer to a cylinder endwall during spin-up/spin-down," *Chem. Eng. Sci.*, **45**, No. 6, 1571–1581 (1990).
9. A. G. Kirdyashkin and V. É. Distanov, "Hydrodynamics and heat transfer in a vertical cylinder exposed to periodically varying centrifugal forces (accelerated crucible rotation technique)," *Int. J. Heat Mass Transfer*, **33**, No. 7, 1397–1415 (1990).
10. Xu Yiu-Bin and Fan Shi-Ji, "Accelerated crucible rotation technique: Bridgman growth of $\text{Li}_2\text{B}_4\text{O}_7$ single crystal and simulation of the flows in the crucible," *J. Crystal Growth*, **133**, 95–100 (1993).
11. Seung Jae Moon, Charn-Jung Kim, and Sung Tack Ro, "Effects of buoyancy and periodic rotation on the melt flow in a vertical Bridgman configuration," *Int. J. Heat Mass Transfer*, **40**, No. 9, 2105–2113 (1997).
12. Liu Juncheng and Jie Wanqi, "Modeling Ekman flow during the ACRT process with marked particles," *J. Crystal Growth*, **183**, 140–149 (1998).
13. V. É. Distanov and A. G. Kirdyashkin, "Modeling of heat transfer in a melt in growing single crystals by the Stockbarger method using the accelerated crucible rotation technique (ACRT)," *Prikl. Mekh. Tekh. Fiz.*, **39**, No. 1, 98–104 (1998).
14. V. É. Distanov, A. G. Kirdyashkin, and B. G. Nenashev, "Forced stirring of the melt during the growth of single crystals by the Bridgman–Stockbarger method," in: *Materials on Genetic and Experimental Mineralogy. Crystal Growth* [in Russian], Nauka, Novosibirsk (1988), pp. 21–42.
15. V. E. Distanov and A. G. Kirdyashkin, "Effect of forced convection on impurity distribution over PbBr_2 single crystals," *Inorgan. Mat.*, **33**, No. 11, 1177–1179 (1997).
16. N. B. Singh, A. M. Stewart, R. D. Hamacher, et al., "Convecto-diffusive growth of lead bromide crystals: A test of theories," *J. Crystal Growth*, **139**, 158–164 (1994).